NUMERICAL SIMULATION OF A HIGH TEMPERATURE THERMAL STORAGE UNIT FOR SOLAR GAS TURBINE APPLICATIONS

Peter Klein[1],Thomas Roos[2], John Sheer[3]

[1] BSc (Eng), Department of Mechanical Engineering, University of the Witwatersrand, Johannesburg 2050, South Africa, peter.klein@students.wits.ac.za

[2] M. Eng. (Mech), Principal Research Engineer, CSIR (DPSS), P O Box 395, Pretoria 0001, South Africa,

[3] Professor, PhD Sc (Mech Eng), Department of Mechanical Engineering, University of the Witwatersrand, Johannesburg 2050, South Africa

Abstract

The implementation of thermal storage systems allows concentrating solar power plants to generate predictable power delivery to the grid by mitigating the variability of solar energy supply. However, while thermal storage solutions exist for Rankine cycles, in the form of molten salts and thermal oil reservoirs, the high temperature nature (>800˚C) of Brayton cycles requires a different approach. One solution is to make use of a high temperature packed bed.

The transient heating and cooling of a packed bed of ceramic pebbles is investigated in the current work through a numerical analysis, with experimental validation. The technique of orthogonal collocation on finite elements is used to solve the governing heat transfer equations for the fluid, solid and wall temperature distributions in two dimensions. Radiation effects are incorporated in the model through the Zehner-Schlünder effective thermal conductivity model and are verified against the SANA test cases with good agreement. Non-uniform radial porosity and velocity distributions are also incorporated and are found to have a notable effect on the temperature profiles. Numerical results are compared to preliminary test results from a packed bed test rig. The heating tests show a good correlation between predicted and measured temperature profiles, while the cooling of the bed is not accurately represented at present. Modifications to the test setup are proposed.

Keywords: High Temperature, Thermal Storage, Wall Channeling, Radiation

1. Introduction

The use of a gas turbine rather than a steam turbine as the prime mover in a solar power station presents at least two significant advantages: the possibility of higher Carnot efficiencies (in combined cycle operation) and a significant reduction in water usage. The latter makes a solar gas turbine an attractive option, as solar power plants are generally placed in arid areas where cooling water is a scarce resource.

However, due to the fact that the turbine inlet temperature on gas turbines is >800˚C, difficulties are encountered when thermal storage is considered. Traditionally, the favoured thermal storage technology is a two tank molten salt system, as incorporated on the Rankine cycle plants at Themis Targasonne in France and Andasol-1 in Spain. [1] These salts are only viable up to temperatures of approximately 500˚C. At higher temperatures they can decompose and thus have not as yet been implemented on gas turbines systems. It is for this reason that alternative thermal storage techniques must be investigated.

Packed beds are well suited to thermal storage applications, as they are characterised by excellent heat transfer characteristics and have a large surface area for heat exchange. In this system, heat is transferred between a bed of spherical solid pebbles, a fluid passing through the bed, and the bed wall. Thermal energy is stored in the sensible heat of the pebbles. Another advantage of packed beds is that a steep thermocline develops during charging and discharging, allowing the system to withdraw heat at the required temperature level, which is vital the operation of a sensible heat thermal storage system. Effective design of a packed bed thermal storage system requires detailed modeling that is able to predict the transient temperature distributions of the fluid and solid phases and the bed wall.

2. Governing Equations for Forced Convection Heat Transfer in a Packed Bed

The governing heat transfer equations are formulated based upon the conservation of energy in the bed. Due to the complexities involved the individual particles are not modeled explicitly. Instead a global bed model is introduced, described by volume averaged transport parameters. An extensive overview of the thermal modeling of packed beds is provided by [2]. In the current work a two dimensional, heterogeneous model is utilised, accounting for the thermal disequilibrium between the fluid and solid phases. Energy equations are presented for both the fluid T_f and solid T_s phases, coupled by an inter-phase heat transfer coefficient. It has been noted by various authors [3] that under transient conditions the thermal capacity of the wall can have a marked effect of the heat transfer in the near wall region of the bed. As it is an aim of the current work to model this region accurately, a third energy equation has been included to model the wall temperature T_w and account for any thermal lag in the bed wall. The governing partial differential equations for heat transfer in the bed are presented below in axisymetric form.

Energy equation for the *fluid* phase:

$$\rho_f c_f \left(\varepsilon \frac{\partial T_f}{\partial t} + u_x \frac{\partial T_f}{\partial x}\right) = \frac{\partial}{\partial x}\left(K_{fx} \frac{\partial T_f}{\partial x}\right) + \frac{1}{r}\frac{\partial}{\partial r}\left(rK_{fr} \frac{\partial T_f}{\partial r}\right) + ha_p(T_s - T_f)$$

Energy equation for the *solid* phase:

$$\rho_s c_s (1-\varepsilon) \frac{\partial T_s}{\partial t} = \frac{\partial}{\partial x}\left(K_{sx} \frac{\partial T_s}{\partial x}\right) + \frac{1}{r}\frac{\partial}{\partial r}\left(rK_{sr} \frac{\partial T_s}{\partial r}\right) + ha_p(T_f - T_s)$$

Energy equation for the *Wall*:

$$\rho_w c_w \frac{\partial T_w}{\partial t} = \frac{\partial}{\partial x}\left(k_w \frac{\partial T_w}{\partial x}\right) + \frac{1}{r}\frac{\partial}{\partial r}\left(rk_w \frac{\partial T_w}{\partial r}\right)$$

3. Evaluation of Working Parameters for Energy Equations

3.1. Void Fraction - ε

Due to the confining effect of the wall on randomly packed particles, non-uniform structural characteristics are introduced into packed beds. The effect of an impermeable boundary causes the location of the packed particles to be restricted leading to radial variations in void fraction. [4] This variation in void fraction in turn affects fluid flow and heat transfer properties and it is therefore included in the current analysis through the profile proposed by Hunt and Tien, [5] where $\varepsilon_\infty$is the void fraction in the core region of the bed and has been set to 0.39.

$$\varepsilon(r) = \varepsilon_\infty \left(1 + \frac{1-\varepsilon_\infty}{\varepsilon_\infty} exp\left(-6\frac{R-r}{dp}\right)\right)$$

3.2. Superficial Velocity Profile - u_x.

The radial variation in void fraction causes a maldistribution of flow in the packed bed. The higher void fraction near to the wall introduces a velocity channeling effect, by which the velocity near to the wall is higher than in the centre of the bed. This channeling profile must be resolved in order to accurately calculate the convective term in fluid energy equation. The flow in this system is predominately axial. In order to save computational time, the radial flow was assumed negligible and only the axial flow was modeled. The axial momentum equation is a Navier-Stokes type equation, which includes the Darcy and Forcheimer terms (Ergun Equation) and the viscous dissipation is given by the Brinkman's expression. [6] The pressure gradient was calculated using the standard Ergun equation and the bulk properties of the packed bed. This equation is solved at each time step n using the calculated temperature field from the previous time step n-1. The global collocation method was utilised with 30 x 30 collocation points to resolve the superficial axial velocity field.

$$\rho\left(\frac{1}{\varepsilon}\frac{\partial u_x}{\partial t}+\frac{u_x}{\varepsilon^2}\frac{\partial u_x}{\partial x}\right)=-\frac{\partial P}{\partial x}-\left(\frac{\mu}{\boldsymbol{K}}+\rho C u_x\right)u_x+\frac{\mu_{eff}}{\varepsilon}\frac{\partial^2 u_x}{\partial x^2}+\frac{\mu_{eff}}{\varepsilon}\left(\frac{\partial^2 u_x}{\partial r^2}+\frac{1}{r}\frac{\partial u_x}{\partial r}\right)$$

where the Ergun coefficients are given by:

$$\boldsymbol{K}=\frac{{d_p}^2\varepsilon^3}{150(1-\varepsilon)^2}\qquad C=\frac{1.75(1-\varepsilon){d_p}^2}{d_p\varepsilon^3}$$

3.3. Effective Solid Thermal Conductivity - K_{sx}, K_{sr}

The effective solid thermal conductivity accounts for heat transfer in the solid phase under stagnant conditions where convective mechanisms are not present. The Zehner-Schlünder [8] model for effective solid thermal conductivity is based upon the theory of a unit cell containing two deformable half particles surrounded by a stagnant fluid. This model has been widely used in the modelling of heat transfer in packed beds. It has also been modified by the International Atomic Energy Agency [9] to include radiation effects. Due the high temperature nature of the current work, this modified form of the ZBS model is utilized in the current work.

The effective thermal conductivity is a function of void fraction and must be adjusted in the near wall region. Visser [7] has proposed a modified radiative component of the model, with results accurate to 12% for a natural convection system. This approach has been followed in the current work.

3.4. Effective Fluid Thermal Conductivity - K_{fx}, K_{fr}

The effective fluid thermal conductivity is a function of the fluid thermal conductivity k_f and the thermal dispersion effect. Thermal dispersion is defined as the transport of heat through the turbulent mixing of the fluid as it flows through the packed bed. The model of Yagi and Kuni [10] is adopted to model the dispersion effect as a linear function of Prandtl number Pr and particle Reynolds number Re_p.

$$K_{fx}=\varepsilon k_f+0.5Re_pPr$$

$$K_{fr}=\varepsilon k_f+0.1Re_pPr$$

$$Re_p=\frac{\rho_f d_p u_x}{\mu_f}$$

3.5. Inter-Phase Heat Transfer - $h\mathrm{a_p}$

This empirical coefficient describes the heat transfer between the solid and fluid phases. The correlation proposed by Gunn [11] is valid for $0.35 \leq \varepsilon \leq 1$ and $\mathrm{Re_p} \leq 10^5$. It can therefore be used to describe inter-phase heat transfer in the near wall region. The term a_p represents the ratio between the superficial particle area and the particle volume

$$Nu_p=\frac{hd_p}{k_f}=(7-10\varepsilon+5\varepsilon^2)\left(1+0.7Pr^{0.33}Re_p^{0.2}\right)+(1.33-2.4\varepsilon-1.2\varepsilon^2)Pr^{0.33}Re_p^{0.2}$$

$$a_p=\frac{6(1-\varepsilon)}{d_p}$$

3.5. Boundary Conditions

The system boundary conditions for the interior of the bed and the bed wall are presented in Figure 1. The radiation boundary condition between the solid and the wall has been linearised through the introduction the coefficient h_r. The term T_{sr} represents the value of the solid temperature at half a pebble diameter from the wall, as suggested by

[7]. The fluid convection coefficient h_w is calculated according to Tsotsas and Schlunder [12].

$$h_r = \sigma\left(\frac{1}{\zeta_s}+\frac{1}{\zeta_w}-1\right)^{-1}(T_{sr}+T_w)(T_{sr}^2+T_w^2) \qquad h_w = 4.05k_f Re_p^{0.5}$$

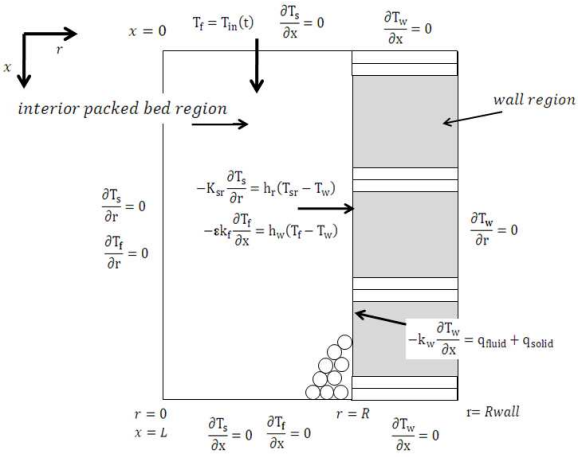

Fig. 1. Boundary conditions for thermal storage model

4. Numerical Solution

The governing heat transfer equations cannot be solved analytically and thus a numerical solution must be sought. The technique of orthogonal collocation on finite elements (OCFE) has been chosen for the current work due to its ability to accurately resolve steep gradients in a problem domain. [13]

4.1. Temporal Discretisation

Temporal discretisation of the governing equations was completed through an implicit finite difference scheme. The terms $\frac{\partial T_f}{\partial t}$, $\frac{\partial T_s}{\partial t}$ and $\frac{\partial T_w}{\partial t}$ were discretised using a second order backward difference operator with a truncation error of $\boldsymbol{\mathcal{O}}(\Delta t)^2$. The temporal discretisation of the fluid phase energy equation is presented below.

$$\rho_f c_f\left(\varepsilon\frac{3T_f^{n+1}-4T_f^{n}+T_f^{n-1}}{2\Delta t}+u_x\frac{\partial T_f}{\partial x}^{n+1}\right) = K_{fx}\frac{\partial^2 T_f}{\partial x^2}^{n+1} + \frac{\partial K_{fx}}{\partial x}\frac{\partial T_f}{\partial x}^{n+1} + K_{fr}\frac{\partial^2 T_f}{\partial r^2}^{n+1} + \left(\frac{K_{fr}}{r}+\frac{\partial K_{fr}}{\partial r}\right)\frac{\partial T_f}{\partial r}^{n+1} + ha_p(T_s - T_f)^{n+1}$$

As the solution of these equations requires the properties of the fluid, solid and wall at time n+1, an iteritive solution procedure is implemented at each time step. The properties at iteration i-1 are used to generate a new temperature field at iteration i. The physical properties are then re-evaluated using this temperature field. This procedure is continued until convergence. The non linear terms are also evaluated in this manner, by numerically differentiating the thermal conductivity (w.r.t x and r) at the previous iteration step i-1

4.2. Spatial Discretisation

Orthogonal collocation forms part of the method of weighted residuals (MWR), of which the well known Galerkin and least squares methods are included. The collocation procedure represents the solution by an Nth order series $\sum_{i=0}^{N} a_i\phi_i$, of smooth basis functions consisting of orthogonal polynomials. This series expansion is known as the trial function and contains (N+1) unknown coefficients that must be determined in order to generate a solution (one dimension). A residual is formed when the trial function is substituted into the differential equation that is to be solved. This residual is forced to be zero at (N+1) collocation points, generating the required number of algebraic

equations to solve for the all unknown coefficients in the trial function. In order to minimise the error, these collocation points are chosen to be the Gauss Lobotto quadrature points given by:

$$x_i = \cos\left(\frac{\pi i}{N}\right) \qquad \text{for i=0,1,...,N}$$

The basis function for the current work is the shifted Chebyshev Polynomials, valid on the domain [0,1]. These polynomials are defined according to the trigonometric identity, $\phi_n(x) = \cos(n\cos^{-1}(2x-1))$. As described by Finlayson [13], the procedure for two dimensional problems is to take the tensor product of two one-dimensional polynomials, one in x and one in r. Thus, for the global collocation method, the unknown temperature is approximated by:

$$T(x,r,t) = \sum_{i=0}^{N_x}\sum_{j=0}^{N_r} a_{ij}(t)\,\phi_i(\boldsymbol{x})\phi_j(\boldsymbol{r})$$

4.2.1 Orthogonal Collocation on Finite Elements

Global collocation methods produce highly accurate solutions, but require the solution to be relatively smooth throughout the domain. In the case of the current problem it is expected that sharp temperature gradients will be present in the near wall region. Steep gradients can lead to oscillations in the solution when global collocation is used. In these cases the technique of orthogonal collocation on finite elements (OCFE) is advocated. Another advantage of this method, in the context of the current work is that it will allow for the accurate modelling of the wall region, as elements can be placed in the flanges of the wall to capture the heat transfer from the flange to the insulation.

In OCFE the problem domain is first discretised into small sub domains, known as finite elements. The orthogonal collocation technique as outlined above is then applied to each element, using a lower order trial function. In the current work a cubic order interpolating polynomial has been used. Continuity of the function and first derivative are imposed on the nodal points on the boundaries between the finite elements. Thus, a piecewise polynomial approximation is utilised instead of a global polynomial approximation. The region 0≤r≤R in Figure 1 represents the interior section of the packed bed. The region R≤r≤Rwall represents the section of the bed wall that has been modelled. The test rig is insulated further than 0.25m but it was found that the heat penetration into the insulation is primarily restricted to this region. The heat flux after it is considered to be negligible.

The shifted Chebyshev polynomials are only valid on the domain [0,1]. The variables x and r are mapped onto this domain through the introduction of two local element variables, α and β.

$$\alpha = \frac{x-x_k}{x_{k+1}-x_k} = \frac{x-x_k}{\Delta x_k} \qquad \text{and} \qquad \beta = \frac{r-r_k}{r_{k+1}-r_k} = \frac{r-r_k}{\Delta r_k}$$

The temperature derivative in the *kl*th element is then approximated using the chain rule.

$$\frac{\partial T^{kl}}{\partial x} = \frac{1}{\Delta x_k}\sum_{i=0}^{3}\sum_{j=0}^{3} a_{ij}^{kl}(t)\frac{\partial \phi_i(\alpha)}{\partial \alpha}\phi_j(\beta)$$

The differential equations are satisfied at each interior collocation point. Collocation points lying on the boundary of the domain satisfy the boundary conditions. Finally the continuity of the function and the first derivative are enforced on the collocation points that lie on the inter element boundaries. At a cross point, where 4 elements share a single point, the sum of normal derivatives in the x and r directions is used. This patching approach must be altered slightly when modelling the wall. In this region the thermal conductivity is either equal to the thermal conductivity of the metal or the insulation. In this case the gradient is discontinuous and the continuity of fluxes must be imposed.

5. Numerical Solution to SANA Test Case

The SANA test cases [14] provide an excellent test case for the efficacy of the radiation correlations, including the linearised solid radiation boundary condition and the modified Zehner-Schlünder effective conductivity model. In this experiment, a central heating element of 35kW was used to heat a closed packed bed to temperatures >1300K. Although a natural convection flow system, at elevated temperatures radiation is the dominant heat transfer mechanism as shown by the narrow spread in the experiment data measured at different axial locations. The numerical model described in Sections 3-4 was used to model the SANA test case with no energy equation for the bed wall, but rather the imposition of boundary conditions. No flow was included and thus the natural convection was not modelled. A radiation boundary condition was assumed on the inner wall and a fixed temperature boundary on the outer wall. It can be seen the model predicts the solid temperature profiles accurately, as shown in Figure 2, lending credit to the radiation correlations, boundary conditions and the numerical procedure.

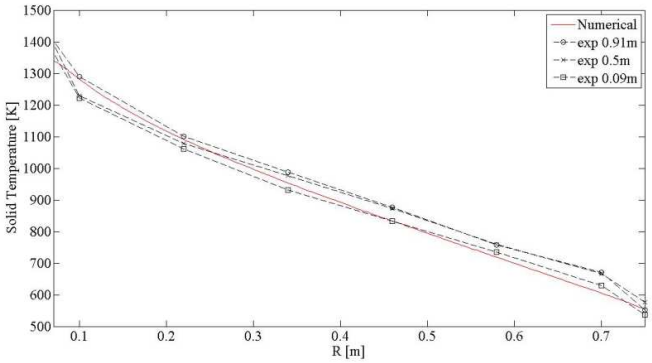

Fig. 2. Numerical and experimental results for SANA test case

6. Forced Convection Test Rig – Numerical and Experimental Results

In order to validate the model under forced convection conditions, a high temperature packed bed test rig has been designed and built (Figure 3a). The bed consists of flanged sections of Nimonic alloy pipe. Each section is 0.2m in length and 0.4m ID. It is packed with Denstone ceramic pebbles of 19mm diameter. At the base of the bed, a rigid steel grating (20mm gap) has been fitted, which creates a support base for a 5mm gap wire mesh upon which the pebbles rest, while allowing the air to freely pass through it.

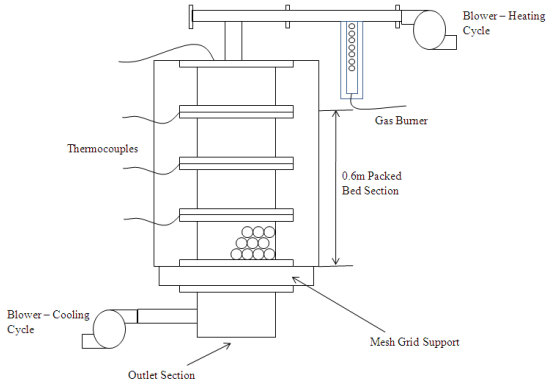

Fig. 3a. Thermal Storage Test Rig

Fig. 3b. Denstone ceramic pebbles

Air is forced through the bed by a blower. The mass flow is calculated using a bellmouth on the inlet section of the blower and a manometer. The heating of the packed bed is achieved using a propane gas burner, installed downstream of the blower. During the charging cycle the heated air from the burner is forced through the bed from

the top inlet by the blower and exhausted out of the base of the bed. During the discharge cycle, the gas burner is shut off and the blower is placed at the base section of the bed. The cold air is then blown through the bed and exhausted out of the top section. In order to measure the temperature of the solid at various positions in the bed, 20mm stainless steel ball bearings are utilised. A K-type thermocouple is inserted into a 5mm hole which has been spark eroded from the surface to the centre of the ball bearing. At present the fluid phase temperature has not been recorded in the bed, only upstream. A grid of ten instrumented pebbles has been placed into the bed at present to measure the solid temperatures. At the completion date of this paper preliminary testing has begun on the test rig at low temperatures (300˚C). These results are presented in Figures 4 and 5.

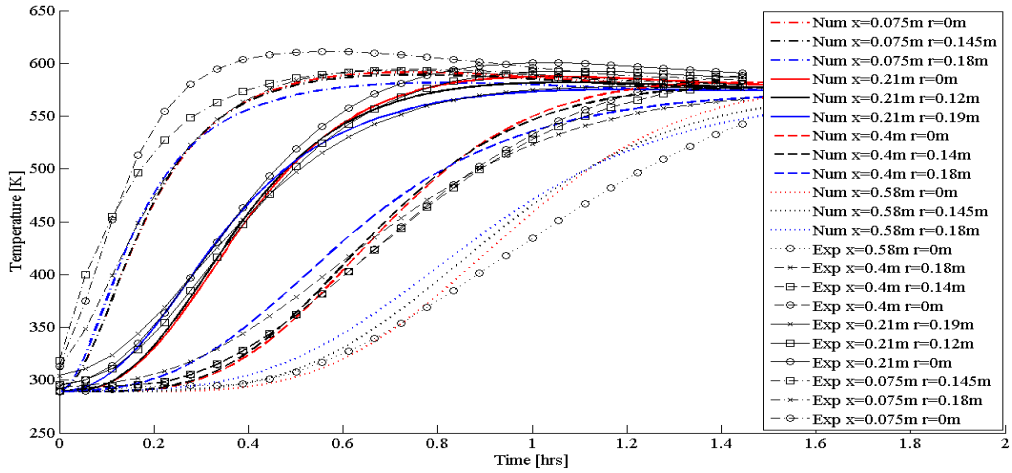

Fig. 4. Comparison between numerical and experimental results for the heating of the packed bed

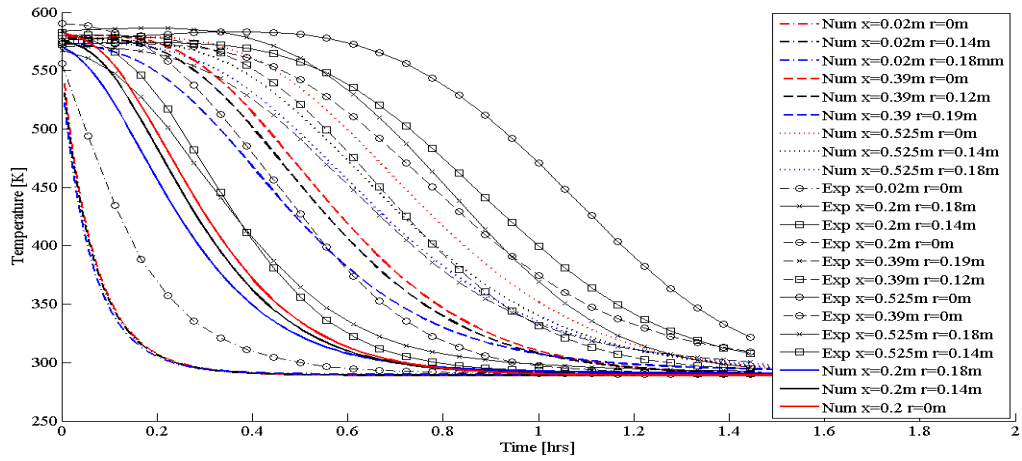

Fig. 5. Comparison between numerical and experimental results for the cooling of the packed bed

7. Discussion

A comparison between the measured and predicted temperature profiles, during the transient heating of the test rig, shows that there is a good correlation between the numerical and experiment data. The numerical model effectively predicts the heating of the packed bed.

The results for the cooling of the packed bed do not show a good correlation between the predicted and measured data. The numerical model is seen to overestimate the cooling. This can be explained by the test rig setup. During cooling, the flow direction is reversed and the air enters the bed from the base of the rig. The numerical model

assumes that the inlet air temperature into the packed bed is at a constant 16˚C. However, the air must pass through the rigid steel grating, prior to entering the bed. This grating has been heated to approximately 300˚C and the data suggests that it has a significant thermal inertia. Thus, the actual inlet air temperature into the bed is much higher than that assumed by the model, resulting in an extended cooling period. The influence of the thermal inertia of the exit section is also shown on the heating curves. The temperature of the pebble placed near to the base of the bed, takes longer to heat than predicted. Future testing will place a thermocouple at the inlet of the packed bed above the steel grid. This will allow the exact inlet temperature to be measured during the cooling of the bed to be applied to the numerical model.

8. Conclusions

The SANA test case has shown that the numerical method described in this paper is able to resolve conduction and radiation effects with encouraging accuracy. The numerical model accurately predicts the heating of the packed bed. The cooling of the bed is over predicted by the numerical model. Modifications must be made to the test rig setup in order to compare the numerical and experimental cooling profiles. Channelling is significant and causes preferential heating and cooling of the outer pebbles in the bed.

References

[1] Renac Presenation on CSP (2009), Thermal Energy Storage, South Africa.

[2] N. Wakao, S. Haguei, (1982). Heat and mass transfer in packed beds, Gordon and Breach, New York.

[3] D.E Beasley, J.A. Clark, (1984). Transient response of a packed bed for thermal energy storage, Int J. Heat and Mass Transfer, 27.9: 1659-1669.

[4] R.F. Benenati, C.B. Brosilow, (1962). Void fraction distribution in beds of spheres. A. I. Ch. E. J 8: 359-361.

[5] M.L. Hunt, C.L. Tien, (1990). Non-Darcian flow, heat and mass transfer in catalytic packed bed reactors. Chemical Engineering Science, 45:55-63.

[6] C.O. Castillo-Araiza, H. Jimenex Islas, F. Lopez-Isunza, (2007). Heat-Transfer in Packed Bed Catalytic Reactors of Low Tube/Particle Diameter Ratio. Ind. Eng. Chem Res, 56: 7426-7435.

[7] C.J. Visser, (2007). Modelling heat and mass flow through packed pebble beds: A heterogeneous volume averaged approach. M.Eng Thesis, University of Pretoria.

[8] P. Zehner, E.U. Schlünder, (1970). Warmeleitfagkeid von schuttungen bei massigen temperaturn. Chem-Ing. Tech. 42: 933-941.

[9] IEAE (2001). Heat transport and afterheat removal for gas cooled reactors under accident conditions. Tech. Rep. IAEA-TECHDOC-1163, International Atomic Energy Agency.

[10] S. Yagi, D. Kunii, (1980). Studies on effective thermal conductivities in packed beds. A.I.Ch.E. Journal 3:373:381

[11] D.J. Gunn, (1978). Transfer of heat or mass to particles in fixed or fluidized beds. International Journal for Heat and Mass Transfer, 21:467-476.

[12] E. Tsotsas, E.U. Schlünder, (1990). Heat transfer in packed beds with fluid flow: Remarks on the meaning and calculation of the heat transfer coefficient at the wall. Chem. Eng. Sci. 45:819:837.

[13] B.A. Finlayson, (1979). Orthogonal collocation on finite elements: Progress and Potential. Advances in computer methods for partial differential equations –II.

[14] H.F. Niessen, B. Stöcker, (1994). Data sets of the SANA experiment. Forschungszentrum Jülich, Germany.